3
Experimental Methodology

3.1 INTRODUCTION

The raw materials and ceramic samples in the present research work were characterized a) quantitatively, b) qualitatively, c) chemically and d) mechanically using various instrumentation techniques to understand the compositional, mineralogical, thermal, morphological, chemical and strength characteristics. The various techniques used are discussed in detail in the following sections below.

3.2 QUANTITATIVE CHARACTERIZATION TECHNIQUE

3.2.1 X-ray Fluorescence

The composition of a material can be investigated using X-ray fluorescence spectroscopy. The composition is expressed quantitatively in terms of ppm or (parts per million) or percentage by weight. Here the atoms can be excited using an external energy source. Once excited these atoms radiate X-rays of a characteristic wavelength.

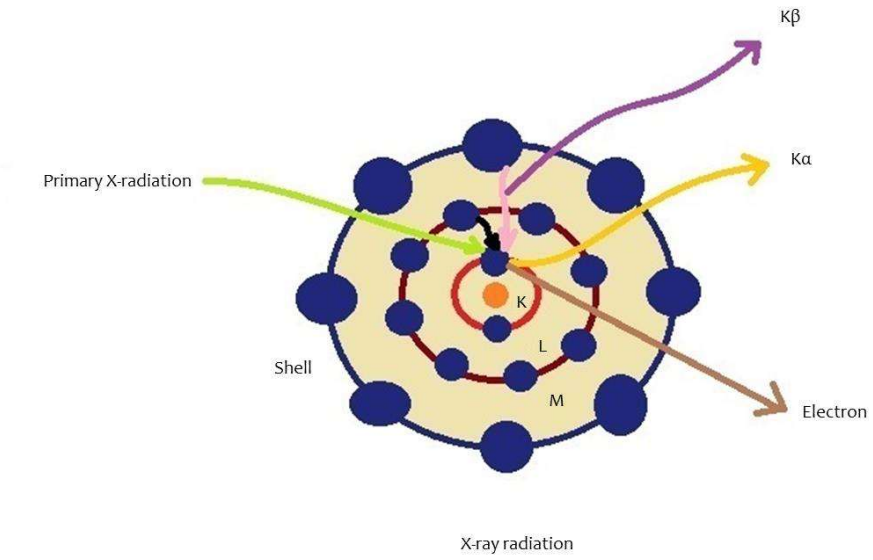

Figure 3-1 : X-ray fluorescence phenomena [*Source:* Pesce *et al*., 1971]

Working Procedure

Three main components of this system are X-ray source, a material sample and a detector system. X-rays produced are named primary and they pass through the monochromator which then is incident on the sample surface. The monochromatic X-rays collide with the atoms of the sample. The X-rays usually knock the electrons out from the inner shell of an atom. To restore the stability of the atom, electrons from higher energy level occupy these vacancies. The energy release takes place in the form of secondary X-rays as the electron transits from high energy level to a lower energy level. These secondary X-rays are characteristic of the element under investigation and are collected and measured by a detector [Norrish and Chappell, 1977]

XRF instrumentation is classified into two types:

Energy dispersive XRF spectrometer (EDXRF)

Wavelength dispersive XRF spectrometer (WDXRF)

In this dissertation, the detection of the chemical composition of raw materials and ceramics is carried using wavelength dispersive XRF spectrometer (**Figure 3-2)**.

Figure 3-2 : X-ray fluorescence instrument AIRF, JNU Delhi

AIRF JNU has a 3D-polarized XRF spectrometer (**Figure 3-3)**. The anode material used is Gd. The filament is of Tungsten.

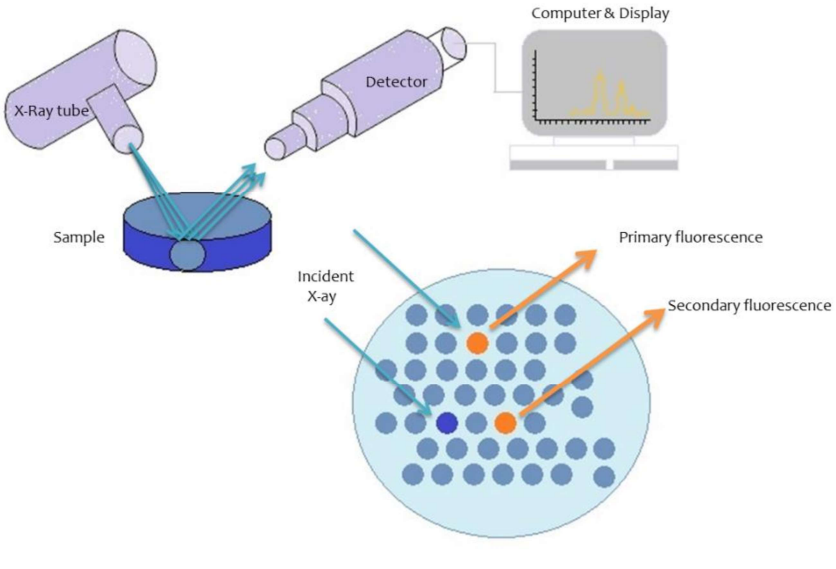

Figure 3-3 : Line diagram of Energy dispersive XRF spectrometer [*Source:* Yeung *et al*., 2003].

The details of the input parameters and sample preparation technique for X-ray fluorescence analysis is been discussed in the subsequent chapters.

3.2.2 X-ray Diffraction (XRD)

The technique is used for mineralogical phase identification in the raw materials and ceramic samples.

X-rays were discovered in 1895 by the German physicist Roentgen and were so named because their nature was unknown at the time. By 1912, the wave nature of X rays was established. The electromagnetic X-ray radiation of short wavelength, are generated during the collision between the high speed accelerated electrons and target metal. The accelerated electrons decelerate in the metal target and as a consequence generate the continuous X-ray spectrum [Borie, 1965]. In this process, some of the high energy electrons knock out the innermost target electrons, generating characteristic X-rays. The radiation emitted by a target includes both types of radiation. In spectroscopic notation, the characteristics radiations are named as Kα, Kβ, Kγ etc. Kα radiation has high intensity and is commonly used for diffraction studies.

Working Procedure

XRD works on the constructive interference of monochromatic X-rays and specimen material (**Figure 3-4)**. Diffraction is a kind of scattering phenomena which satisfies the Bragg's condition [Cullity, 2001].

$$n\lambda = 2d\,sin\theta \tag{3.1}$$

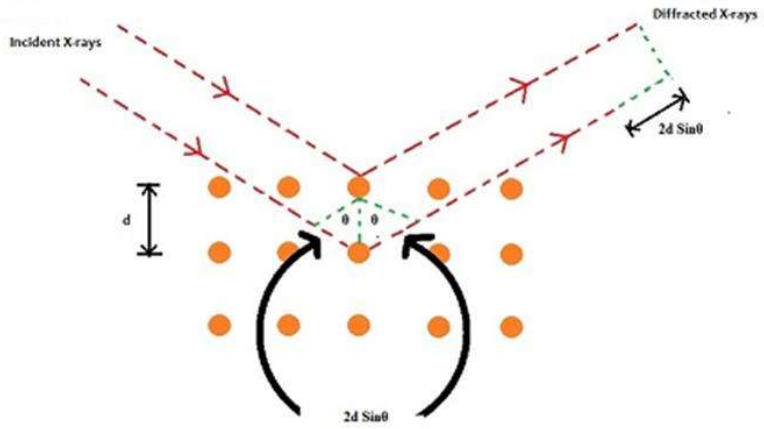

Figure 3-4 : Constructive interference and diffracted rays [*Source:* Cullity, 2001]

XRD instrument consists of three basic elements: an X-ray tube, a sample holder, and an X-ray detector (**Figure 3-5)**.

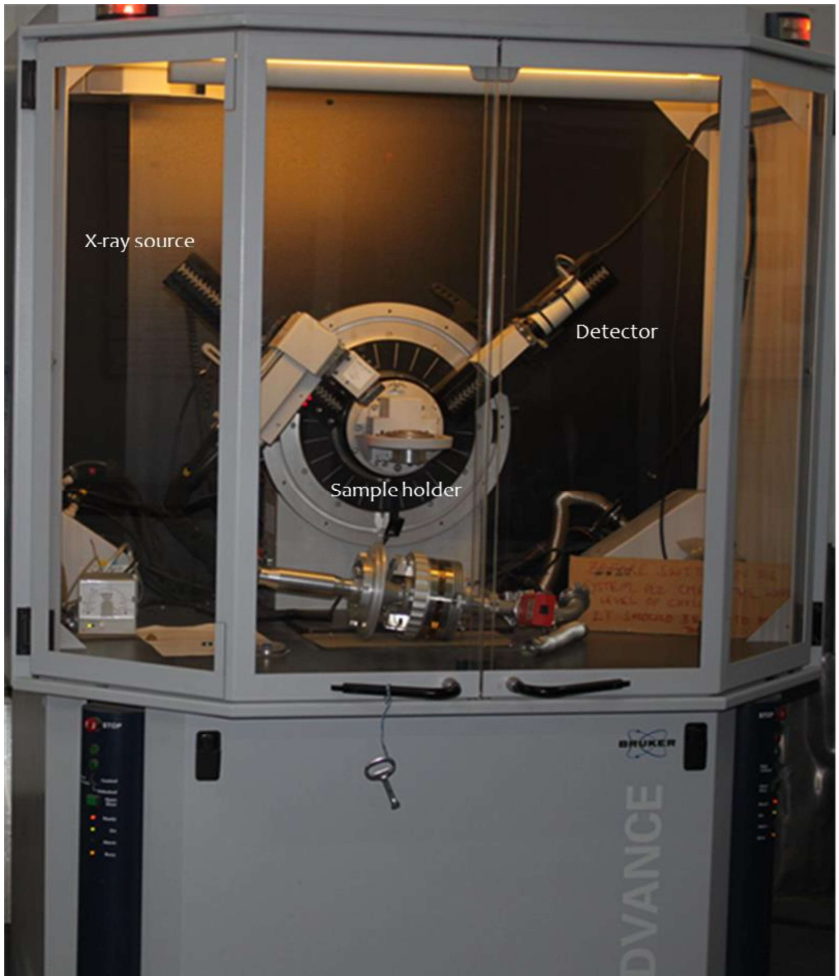

Figure 3-5 : Bruker's X-ray Diffraction D8-Discover instrument at IIT Jodhpur

X-rays are produced in a CRT (cathode ray tube) by heating a wolfram or tungsten filament to produce electrons. The electrons thus produced are accelerated towards the material sample by applying a voltage across the beam of these electrons. The accelerated electrons have sufficient energy to disengage inner shell electrons of the target atom, producing a characteristic X-ray wavelength which is a characteristic of that atom. This spectra commonly has Kα and Kβ wavelengths. K_{α} consists, of $K_{\alpha 1}$ and $K_{\alpha 2}$. $K_{\alpha 1}$ has a shorter wavelength than $K_{\alpha 2}$. The intensity of $K_{\alpha 1}$ is twice that of $K_{\alpha 2}$. These wavelengths are characteristic of the common target materials such as Cu, Fe, Mo, and Cr. Cullity, 2001 reports that crystal-based monochromators are usually required to produce X-rays required in diffraction tests.

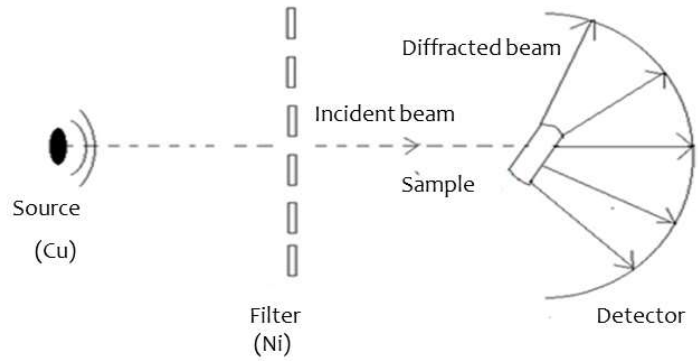

Figure 3-6 : Line diagram of X-ray diffraction instrument working [*Source:* Cullity, 2001]

Copper is the most common target material for single-crystal diffraction, CuKα radiation has a wavelength of 1.5418Å. These X-rays are collimated and directed onto the sample. As the sample and detector are rotated, the intensity of the reflected X-rays is recorded. When the geometry of the incident X-rays impinging the sample satisfies the Bragg equation, constructive interference occurs and a peak in intensity occurs. A detector records and processes this X-ray signal and converts the signal to a count rate which is then output to a device to computer monitor [Cullity, 2001].

In this dissertation work, the minerals present in raw materials and phases evolved during sintering of ceramics were identified by using X-ray powder diffraction (XRD) at room temperature D8 Advance Powder X-ray diffractometer using CuK1 radiation (= 1.54056 Å) as the X-ray source. The phase identification was done by analyzing the XRD data with the standard Joint Committee on Powder Diffraction Standards database (JCPDS).

3.2.3 Fourier Transform Infrared Spectroscopy (FTIR)

Fourier transform infrared (IR) spectroscopy is used to understand the structure of different chemical compounds in the sample. It works on the fact that molecules absorb light in the infra-red region of the electromagnetic spectrum and these molecules are identified by their characteristic vibrational modes [Smith, 2011].

Working Procedure

A beam of IR radiation is directed into the interferometer. The interferometer consists of a beam splitter and a pair of mirrors orthogonal to each other; this produces an interferogram which stores information about the IR radiation at all frequencies simultaneously. When the radiation arrives at the sample some frequencies are absorbed by the sample, some are allowed to pass or be transmitted through the sample. When the transmitted radiation arrives at the detector, information about that radiation is decoded using a mathematical technique called a Fourier transformation. This transmitted wavelength is decoded using Fourier transformation and studied to infer the chemical evolution of the material. The computer software (opus 7.5) produces a graph of percentage transmittance against wavenumber or frequency. This graph is called the IR spectrum of the sample is used for interpretation of the results [Smith, 2011].

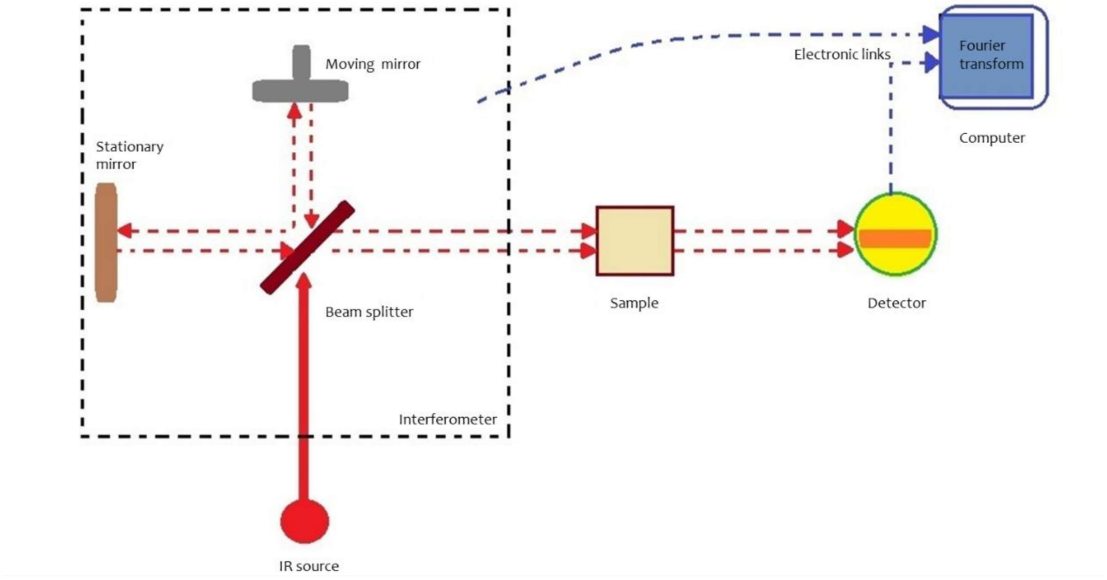

Figure 3-7 : Line diagram showcasing FTIR working principle [*Source:* Smith, 2011]

In this dissertation, Bruker FTIR spectrometer vertex 70v was used and its image is shown in **Figure 3-8**

Figure 3-8 : Bruker FTIR spectrometer vertex 70v, IIT Jodhpur

This spectrometer consists of a room temperature Deuterated and L-alanine doped Triglycine sulfate (DLaTGS) detector. The resolution of this FTIR spectrophotometer is ~ 0.4 cm-1. The powdered ceramic sample was used with potassium bromide in the ratio of 1:10 and the sample was grounded uniformly with KBr until it was uniformly distributed throughout the KBr. The uniform mixture was then pressed into a pellet. The pellet was put on the rack that goes into the light path (inside the IR instrument) and the light shines directly through there. The spectra can be directly read then. Transmittance spectra of the of the ceramic samples were recorded in 400-4000 cm^{-1} wavelength range to understand the evolution of the chemical profile of the sintered ceramics.

3.2.4 Mercury Intrusion Porosimetry (MIP)

It is a powerful technique that allows determining the porosity of materials. One of the biggest advantages of this technique is that it can measure pore sizes in a wide range from few nanometers to several hundreds of microns.

Mercury is a non-wetting liquid and it has a contact angle of greater than 90 degrees. In order for mercury to intrude into a pore, a pressure must applied. As this applied pressure is increased, the mercury is forced into smaller and smaller pores. The applied pressure required to intrude mercury into a pore is inversely proportional to the size of the pore. By increasing the pressure in appropriate increments, the volume of mercury intruded into the pores can be

measured at a range of pressures. From this, an intrusion curve of pore size against intrusion pressure is generated.

The intrusion pressure against volume data is converted to corresponding pore sizes by applying Washburn's equation as shown [Fisher and Lark, 1979].

$$D = \frac{1}{\rho}\, 4Y cos\phi \qquad (3.2)$$

Where D is the pore diameter in microns, γ is the surface tension of mercury, ϕ is the contact angle of mercury and P is the applied pressure in psi.

By knowing the contact angle and surface tension of mercury means that by precisely controlling and measuring the applied pressure the corresponding pore sizes can be calculated.

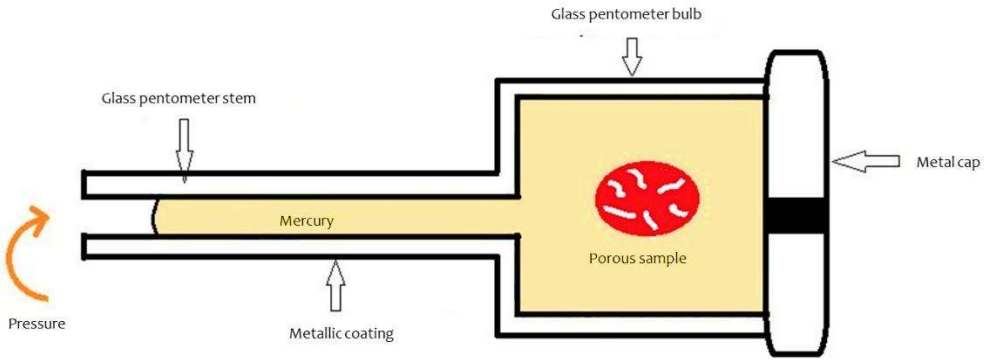

Figure 3-9 : Line Diagram of MIP instrument [*Source:* Abell *et al.*, 1999]

The sample is loaded into a penetrometer for analysis. The penetrometer is made of glass. The penetrometer is sealed with a metal cap when the sample has been loaded. The other end of the cylinder extends into a glass stem with a precisely known volume and is coated with a metallic film.

At the start of the analysis, the penetrometer is evacuated usually to below 50-micron pressure. And the penetrometer is then backfilled with mercury. In the beginning of the analysis, the sample is within mercury. The bulb is full of mercury and the stem is filled with mercury. The volume of mercury held in the stem is essentially a reservoir which is used for intrusion into pores within the sample. As the applied pressure is increased to a point mercury intruded into pores. Mercury moves along the stem and its movement is measured by changes in electrical capacitance. To intrude into pores of 3 nm, a pressure of 60,000 psi must be applied [Berodier *et al.*, 2016].

Working Procedure

The sample of size 3 mm × 3 mm is weighed and put it into the bulb. Seal the open end around the flange with high vacuum grease. The metal cap is kept on the grease and seal it all up with a plastic collar. This assembled penetrometer with the sample inside it is quickly tightened and the sample is ready for analysis on the auto pore.

The analysis is divided into two parts, one at low-pressure and the other at high- pressure. In the configuration, there are 4 low-pressure ports across the top and two high pressure ports placed below the low pressure ports.

The low-pressure analysis starts and the pressure is increased from below atmospheric pressure to above atmospheric pressure. And this increase is undertaken by using a gas cylinder. The ending pressure of the low pressure analysis is very much dependent on the sample morphology (whether it's powder, solid, granular etc). At the end of the low-pressure analysis, penetrometer is taken out. The sample is weighed in order to measure bulk density, volume porosity. The geological samples often have a porosity within the low pressure region and therefore such samples often have low pressure intrusion.

The sample is then loaded into one of the high-pressure ports. The pressure is then increased from the final pressure of the low-pressure analysis up to 60,000 psi

In this dissertation, Porosimeter AutoPore IV from the chemical engineering department at I.I.T Bombay is been used to characterize the percentage porosity and pore size distribution in sintered ceramic samples.

3.2.5 X-ray Micro-computed tomography (X-ray u-CT)

MicroCT is a nondestructive technique of investigating the internal and external structures of a sample without any sample preparation.

Working Procedure

The results are obtained using a three-component system of source, detector and software system obtained are at high resolution [Agrawal *et al*., 2015].

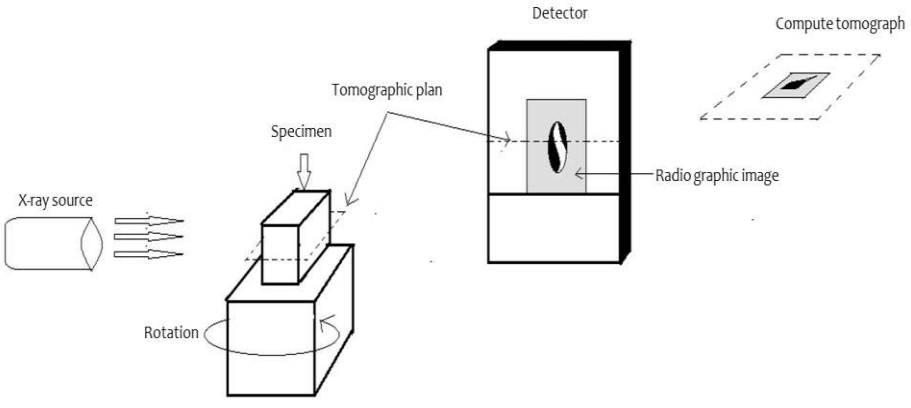

Figure 3-10: Line diagram of Micro-tomography working [*Source:* Agrawal *et al*., 2015]

X-ray source: The x-ray source, scans samples to access internal geometry and failures such as porosity, with high resolution or voxel size. Comparative to conventional testing x-ray

sources, synchrotron-based devices generate narrower X-rays which improves accuracy and detectability [Agrawal *et al*., 2015].

Computerized detector: The detector is placed on the opposite side of the x-ray source. All radiation is directed toward the recording medium. The test object is placed between the x-ray source and the detector panel. A detector panel is commonly a CCD camera, which captures and transforms the x-ray energy into a set of 2D cross-sectional images. The images captured are at predetermined increments, as the object rotates 360 degrees.

Software: A software is utilized to analyze the data and images captured by the detector. It helps to reconstruct two-dimensional layers or slices through the object. By stacking these slices together in an array, it is possible to visualize the structure in three dimensions.

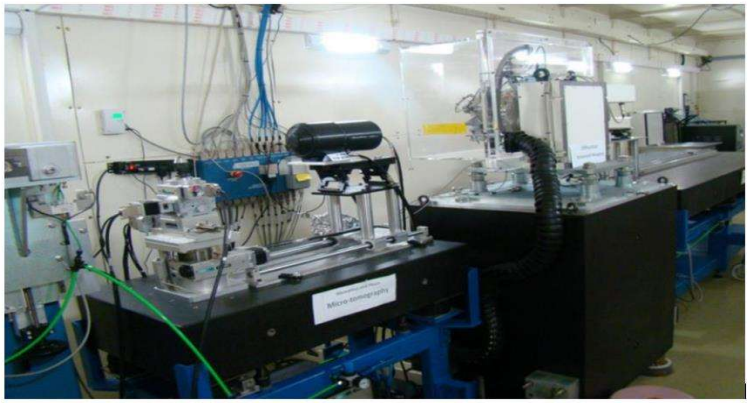

Figure 3-11 : MicroCT instrument at BL-4 RRCAT Indore

The tomographic imaging facility by X-ray synchrotron is located at imaging beamline (BL-4), at RRCAT, Indore [Agrawal *et al*., 2015]. The technical details are tabulated in **Table 3-1**

Table 3-1 : Technical parameters synchrotron-based micro-computed tomography technique (BL-4 Indus 2, RRCAT Indore, India operating at 2.5 GeV, 200 mA.

Components	Typical values
X-ray source	Magnet (bending), 1.5 T dipole
Operation mode	White or monochromatic
Lens	Silicon (111) Double crystal
Energy	8-35 KeV
Material Sample Stage	Five-axis
Sensors	CCD detector or Flat panel detector. Or Photodiode etc.

3.3 MICROSTRUCTURAL CHARACTERIZATION TECHNIQUES

3.3.1 Scanning Electron Microscopy (SEM)

A beam of electrons is incident on a material specimen under study. The study of material surface, cracks, flaws or fissures, and roughness, are the main intention. Electron microscopes were developed to overcome the deficiencies due to low magnifications of microscopes. The first scanning electron microscope (SEM) was commercialized in 1965[Goldstein *et al.*, 2003].

The characteristic features retrieved from scanning electron microscopic images are:

a) The visual appearance, its texture and basic topology of the sample can be studied to establish its relation with material properties.

b) The shape, size and particle distribution over the surface of the sample can be analyzed to associate it with the material properties and behavior.

c) The elements and compounds present in the sample can be identified using energy dispersive spectra (EDS detector coupled with SEM).

The combination of these characteristics along with higher magnification, larger depth of field, and greater resolution makes the SEM one of the most widely used instruments in academic, research areas and industry.

Figure 3-12 illustrates the line diagram of various components of SEM.

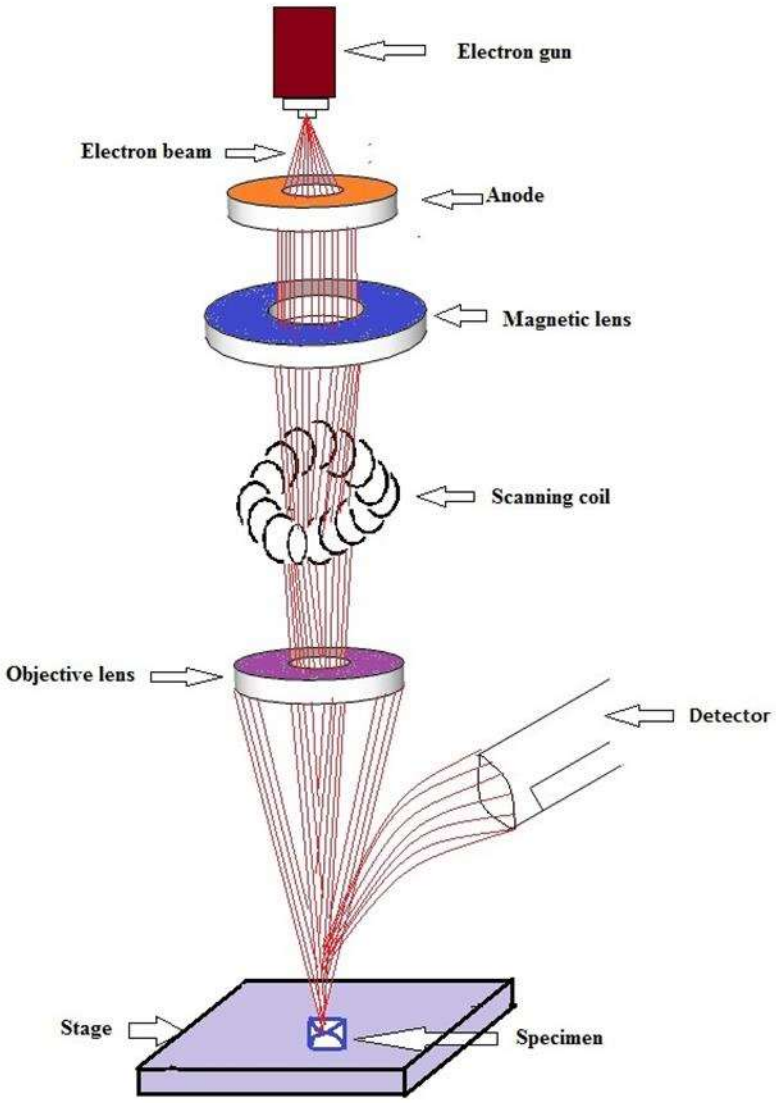

Figure 3-12 : Line diagram of SEM instrument [*Source:* Goldstein *et al*., 2003]

The electron gun produces a stream of electrons emanating from a small spot. Thermionic wolfram, LaB_6, and hot and cold field emission are the sources of electrons. A wolfram or tungsten filament is heated to high temperatures to allow thermionic emission of electrons. Temperatures as high as 2500- 3000^{o}C is required.

Carl Zeiss SEM EVO 18 special edition has been used to analyze the surface and cross-sectional morphologies of ceramics.

3.4 MECHANICAL CHARACTERIZATION

Laboratory-based Universal testing machine (Model EZ-50, Lloyd Instruments, Germany) was used to test the mechanical performance of sintered ceramic briquettes. 3-point bend test and compressive strength tests were carried on the same machine by changing the jaw set up.

3.4.1 Flexural Strength Tests

The series of three-point bend test was conducted on sintered samples prepared. The un-notched samples prepared were of dimensions 100 mm x 15 mm x 15 mm. The span length was kept as 75 mm on the three-point bend universal testing platform (Model EZ50 Lloyd instrument, Germany). ASTM C99/C99M standard test procedure followed to investigate the flexural strength of the specimen. The load application is monotonic loading which is continued till the cracks formed cause separation of samples in parts. The loading rate was maintained at 0.1 Ns^{-1}. The test was carried out at ambient conditions of 300 K and a relative humidity of 40%. For the ceramic samples considered for flexural test flexural stress σ_f was calculated using the following formula [Plappally *et al*., 2010].

$$\sigma_f = \frac{3F_Q L}{2BW^2} \tag{3.3}$$

Where F_Q is the load at the onset of failure L, B and W are the is the distance between the support points, the breadth and width of the sample specimens respectively.

Figure 3-13 : Horizontal placement of ceramic sample over three points [*Source:* Plappally *et al*., 2011]

3.4.2 Compressive Strength Tests

The compression test was carried out on the universal testing platform (Model EZ50 Lloyd Instrument, Germany) using a compression fixture. The size of the test samples was 35 mm x 15 mm x 15 mm. A loading rate of 0.1 Ns^{-1} was applied to the failure of the sample. Test results of compression test were digitally recorded using the data acquisition enabled universal testing platform. The failure occurs when a limiting value of stress is reached equivalent to

$$\sigma_c = \frac{F_q}{A_0} \tag{3.4}$$

Where σ_c is the compressive strength, F_q is the force at the onset of failure and A_0 is the initial cross-sectional area of the sample [Flin, 2007].

Figure 3-14 : Representation of clay ceramic sample under compressive force [Source: Plappally *et al.*, 2011]

3.4.3 Fracture Toughness Experiment

Pre-cracked sintered ceramic specimens of size 100 mm x 25 mm x12.5 mm were loaded monotonically at 3 Ns^{-1} on a UTM machine (Model EZ50 Lloyd Instrument, Germany). The pre-crack length to width ratio (a/W)is maintained at 0.4 for these experiments, where 'a' is (depth of the pre-crack). The loading span was taken to be 80 mm fracture toughness, K_{I_c} was determined from the following expression of ASTM E-399 standard [Soboyejo, 2003; Azeko *et al.*, 2015a].

$$K_{I_c} = f\left(\frac{a}{W}\right) Y_f \sqrt{\pi a} \tag{3.5}$$

Where,

$$\left(\frac{a}{W}\right) = \frac{3\left(\frac{a}{W}\right)^{0.5}\left[1.99 - \left(\frac{a}{W}\right)\left(1 - \frac{a}{W}\right)\left(2.15 - 3.93\frac{a}{W} + 2.7\frac{a^2}{W^2}\right)^{1.5}\right]}{2\left(1 + 2\frac{a}{W}\right)\left(1 - \frac{a}{W}\right)^{1.5}} \tag{3.6}$$

3.5 SURFACE CHARACTERIZATION

3.5.1 Non-Contacting Optical Profilometer

Non-contact optical profilometer traces the surface topography and quantifies the roughness without damaging the actual surface features. It utilizes optical light interference principles to scan and quantify topographic features of various materials ranging from hard ceramics/metals to soft polymers or biological cells.

Working Procedure

The instrument works on the principle of white light interferometry [Vorburger and Teague, 1981] which is shown through line diagram in **Figure 3-15**

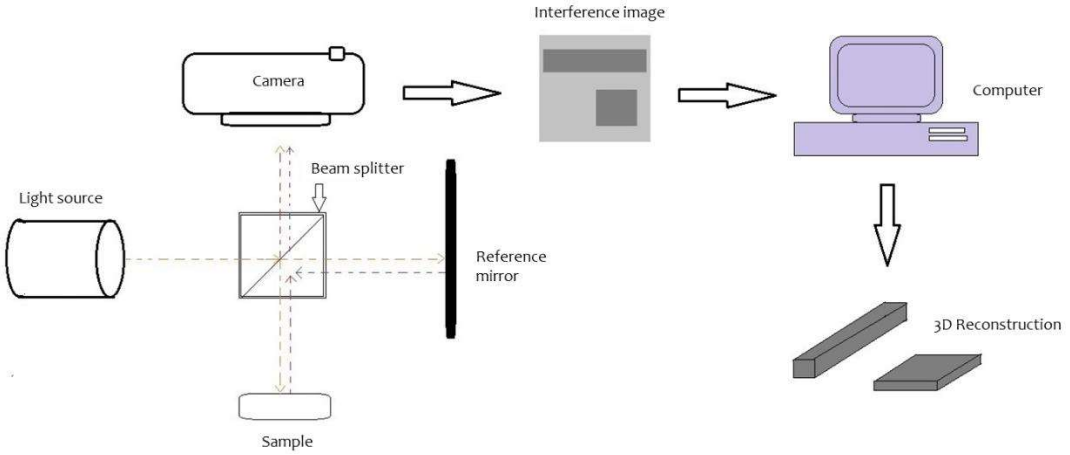

Figure 3-15 : Line diagram of working of Profilometer [*Source:* Rosenfeld and Zanoni, 1975]

The beam of light coming out of the single white light source is split into two by a beam splitter. One half of the beam (reference beam) goes to the reference mirror and reflected by it. The other half of beam (measurement beam) is incident on the test sample and reflected by the sample. These two beams are recombined back by the beam splitter to interfere and light is collected in the CCD. The imaging lens images the interferogram onto the CCD camera. In an ideal case, if the sample and the reference mirror exactly the same then the path difference would be zero, and only bright light will be seen in the CCD. But in reality this is not the case, the surface is different from the reference mirror (there are surface roughnesses) this creates optical path differences. This creates optical interferences and from these various data (parameters) can be calculated. During the vertical scan, the interference patterns are captured by the camera, while the software computes the topography from this data [Vorburger and Teague, 1981].

By changing the position of objective, we change the focus position and thereby the interference fringes also change with surface height from the top surface of the sample to the bottom of the sample. These fringes are collected and the sample surface is re-created.

Important features of non-contact profilometer (Bruker GT-KO) located at Advanced Center for Materials Science (ACMS) are:

- Green Light Source as standard (high resolution imaging) + White Light Interferometry.
- Spatial Sampling of 40 nm. Up to 0.3 - 0.5 µm lateral resolution
- Objectives of 50X + 2X Zoom lens + High Resolution Camera (1280 X 960 pixels).
- Maintains the same pixels to provide high resolution images even at high magnification.
- Can work in both phase-shift mode and vertical-shift mode. Advanced software included stitching images into a large collage.
- Can work in very wide environment conditions.

In this dissertation, the instrument is used to find the surface roughness of the clay ceramic samples to comment on their correlation with the mechanical strength.

3.6 CHEMICAL CHARACTERIZATION

3.6.1 Atomic Absorption Spectroscopy (AAS)

AAS was invented in 1955 by Alan Walsh in Australia. It was first used for mining, medical treatment and agriculture. It is a spectro-analytical technique which is been used to detect trace elements, the concentration of heavy metals or particular metals present in low concentrations typically in the parts per million or parts per billion ranges [Van Loon, 2012]

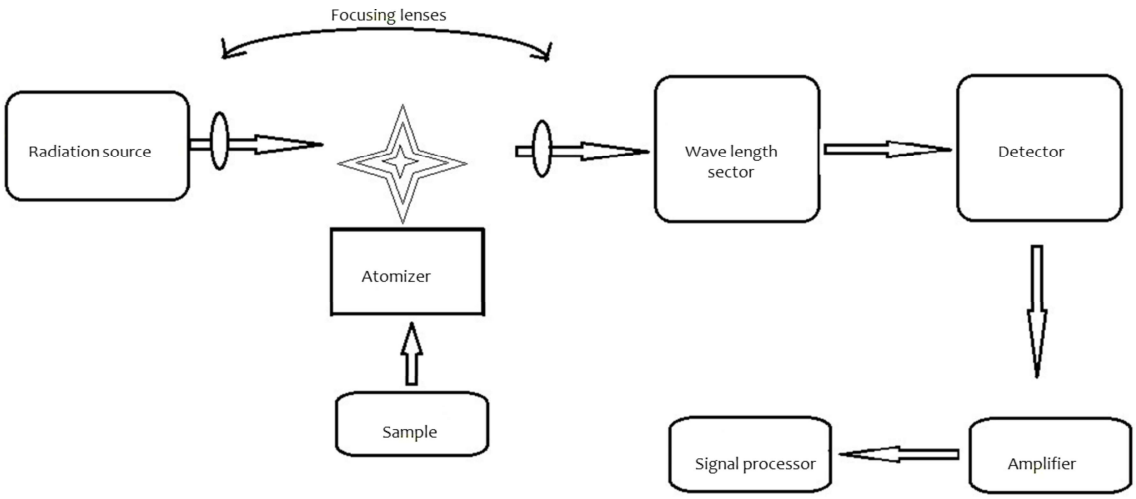

Figure 3-16 : Line diagram of AAS instrument working [*Source:* Van Loon, 2012]

Working Procedure

It is based on the principle of absorption of radiation by free atoms generated in the atomizer. The atoms from a specific element consist of energy levels and there are different from the energy levels of other elements in the periodic table. The energy gap between the energy levels in one atom is different from other atoms of the different elements. If an electron is at a low energy level is provided with some extra energy it will move from low energy level to high energy level. This transition will take place by an absorption of energy. This amount of energy absorbed is a characteristic of energy levels of each atom. In this, the focus is on the amount of energy absorbed during excitation of an electron from one energy level to another. The analyte concentration is determined from the amount of absorption [Van Loon, 2012].

AAS set up (**Figure 3-16)** consists of -

Light source: Hollow cathode lamp is the most common radiation source. It includes a tungsten anode and hollow cylindrical cathode made from the element of interest.

Nebulizer : It converts liquid samples in mist form.

Atomizer: Elements to be analysed needs to be in an atomic state. Atomization involves separation of particles into individual molecules and breaking molecules into atoms. Therefore, compounds constituting the specimens are broken into free atoms at high temperatures using atomizers.

Monochromator: It is also known as a wavelength selector. It selects the specific wavelength of light which is absorbed by the sample and excludes the other wavelengths. It converts the polychromatic light into monochromatic light.

Detector: It converts the electromagnetic waves into electricity.

Concentrations are measured from the working curve after calibrating the instruments with standards of known concentration. Graphs are drawn on the basis of two variables, of which one is set at known values and other is measured as response value.

Figure 3-17 : AAS 500 spectrophotometer at MRC, MNIT Jaipur

…